NeuroImage: Clinical 41 (2024) 103540

Contents lists available at ScienceDirect

NeuroImage: Clinical

journal homepage: www.elsevier.com/locate/ynicl

Brain microstate spatio-temporal dynamics as a candidate endotype of consciousness

Piergiuseppe Liuzzi [a,b], Andrea Mannini [a], Bahia Hakiki [a,*], Silvia Campagnini [a], Anna Maria Romoli [a], Francesca Draghi [a], Rachele Burali [a], Maenia Scarpino [a], Francesca Cecchi [a,c], Antonello Grippo [a]

[a] IRCCS Don Carlo Gnocchi ONLUS, Firenze, Italy
[b] Istituto di BioRobotica, Scuola Superiore Sant'Anna, Pontedera, Italy
[c] Dipartimento di Medicina Sperimentale e Clinica, Università di Firenze, Firenze, Italy

ARTICLE INFO

Keywords:
Brain Spatio-Temporal Dynamics
EEG microstates
Prolonged Disorder of Consciousness
Severe Acquired Brain Injuries

ABSTRACT

Consciousness can be defined as a phenomenological experience continuously evolving. Current research showed how conscious mental activity can be subdivided into a series of atomic brain states converging to a discrete spatiotemporal pattern of global neuronal firing. Using the high temporal resolution of EEG recordings in patients with a severe Acquired Brain Injury (sABI) admitted to an Intensive Rehabilitation Unit (IRU), we detected a novel endotype of consciousness from the spatiotemporal brain dynamics identified via microstate analysis. Also, we investigated whether microstate features were associated with common neurophysiological alterations. Finally, the prognostic information comprised in such descriptors was analysed in a sub-cohort of patients with prolonged Disorder of Consciousness (pDoC). Occurrence of frontally-oriented microstates (C microstate), likelihood of maintaining such brain state or transitioning to the C topography and complexity were found to be indicators of consciousness presence and levels. Features of left–right asymmetric microstates and transitions toward them were found to be negatively correlated with antero-posterior brain reorganization and EEG symmetry. Substantial differences in microstates' sequence complexity and presence of C topography were found between groups of patients with alpha dominant background, cortical reactivity and antero-posterior gradient. Also, transitioning from left-right to antero-posterior microstates was found to be an independent predictor of consciousness recovery, stronger than consciousness levels at IRU's admission. In conclusions, global brain dynamics measured with scale-free estimators can be considered an indicator of consciousness presence and a candidate marker of short-term recovery in patients with a pDoC.

1. Introduction

Severe acquired brain injuries (sABIs) are characterized by traumatic, anoxic, vascular, or other etiology that cause coma for at least 24 h. sABI frequently lead to permanent sensorial, motor, cognitive, or behavioral disabilities with an incidence between 10 and 15 new cases/100,000 persons/year (Masson et al., 2001). After a sABI, some patients may survive in a state of prolonged disorder of consciousness (pDoC). Such condition includes the Unresponsive Wakefulness Syndrome (UWS, eyes open with no evidence of voluntary behaviors (Hirschberg and Giacino, 2011) and the Minimal Consciousness State (MCS), an intermediate state in which minimal, inconsistent but reproducible signs of behavioral responsiveness are present (awareness) (Giacino et al., 2002). Some of these patients may indeed recover full consciousness, whenever a reliable "yes/no" communication is achieved (emergence from MCS, eMCS). Overall, clinical improvement and survival in patients with sABI are commonly associated with neurological severity (Edlow et al., 2020; Whyte et al., 2009); however, high clinical complexity and a vast number of comorbidities (Estraneo et al., 2020; Liuzzi et al., 2022) may also reduce the likelihood of reaching favorable

Abbreviations: sABI, severe Acquired Brain Injuries; MCS, Minimal Consciousness State; UWS, Unresponsive Wakefulness Syndrome; pDoC, prolonged Disorders of Consciousness; CRS-R, Coma Recovery Scale-Revised; GFP, Global Field Power; ICA, Independent Component Analysis; PCA, Principal Component Analysis; GEV, Global Explained Variance; DAN, Dorsal Attention Network; DMN, Default Mode Network.

* Corresponding author at: IRCCS Fondazione Don Carlo Gnocchi ONLUS, via di Scandicci 269.
E-mail address: bhakiki@dongnocchi.it (B. Hakiki).

https://doi.org/10.1016/j.nicl.2023.103540
Received 18 May 2023; Received in revised form 2 October 2023; Accepted 9 November 2023
Available online 16 November 2023

outcomes. Nevertheless, given the heterogeneity of aetiologies and structural lesions leading to a pDoC and the possibility of covert cognition in absence of behavioral response (Thibaut et al., 2021), current guidelines advocate for a multimodal assessment of consciousness combining instrumental techniques (EEG, PET, fMRI) and clinical evaluation (CRS-R) to complement diagnosis (Giacino et al., 2014; Kondziella et al., 2020). Within this context, EEG-based active paradigms have been developed to detect signs of awareness during different tasks (Sitt et al., 2014; Boly et al., 2011) and provide prognostic indicators in pDoC patients (Leon-Carrion et al., 2009; Haveman et al., 2019). Nevertheless, such active paradigms are dependent on higher-order cognitions, thus possible only in MCS + and eMCS (Aubinet et al., 2020; Aubinet et al., 2019). Lastly, these hypothesized proxies of awareness may not be evident in patients without clear neurobehavioral response (Fischer et al., 2010; Wijnen et al., 2007; Kotchoubey, 2005; Kotchoubey et al., 2005). Therefore, when deriving diagnostic and prognostic markers in pDoC patients, data collection protocols should be independent from the intrinstic integrity of the sensorimotor pathways.

To this extent, an EEG spectrum shifted toward higher frequencies (α) (Sitt et al., 2014; Liuzzi et al., 2022; Scarpino et al., 2019) with higher temporal and spatial complexity (resting state and stimuli-related) (Sitt et al., 2014; King et al., 2013) is related to milder alterations of consciousness (Sitt et al., 2014; Chennu et al., 2017; Chennu et al., 2014). Furthermore, it has been highlighted how the presence of a pDoC is mostly related to the disconnection of different cortical regions, rather than to the dysfunction of a single brain area (Chennu et al., 2017; Chennu et al., 2014; Demertzi et al., 2015; Varley et al., 2020; Forgacs et al., 2017). Therefore, there is the necessity to investigate neural functioning looking at the brain as a whole, even if data is sampled electrode-wise (Dipasquale and Cercignani, 2017; Forgacs et al., 2015). In the last years, this concept has been applied to patients with a pDoC via graph theory networks, highlighting impaired network integration and increased network segregation (Chennu et al., 2017; Chennu et al., 2014; Rizkallah et al., 2019). Also, functional connectivity studies reported how information processing in pDoC moves from a global-network mode to a local, single-area data processing (Rizkallah et al., 2019).

Such evidence reflects a disconnection in the thalamo-cortico-thalamic circuit interrupting macro-scale interactions, allowing for single-area properties to determine the global spectral dynamics (Schiff, 2010; Schiff, 2016; Panda et al., 2022). Viewing thalamic activity as a central brain clock, the ABCD model was developed, defining precise operating regimes in terms of bandwidth, spatial distribution of activations and structure for each of the four (A, B, C, or D) EEG labeling (Alkhachroum et al., 2020; Comanducci et al., 2020; Forgacs et al., 2022). Despite the ABCD model providing a classification of brain activity inclusive of the spatial distribution of band-specific activity across the scalp, it does not take into account the transitions between brain states and the spatio-temporal evolution of brain attractors. (Giacino et al., 2014; Boly et al., 2008) A number of theories proposed a parcellation of consciousness in discrete brain states (Bréchet and Michel, 2022; Efron, 1970; Bressler, 1995; Deco et al., 2011; Lehmann et al., 2005; Lehmann, 1990). Lehmann, already from 1987 (Lehmann, 1990; Lehmann, 1995), suggested that discrete brain states could be defined by short-lasting stable global patterns, i.e., “microstates of cognition” or “atoms of thoughts”. Therefore, microstates are short periods (~100 ms) of stable (in topography) EEG potential while varying in strength and polarity. The topology of the main maps (then termed A, B, C, D) was found to be highly reproducible within and across subjects. (Koenig et al., 2002; Michel and Koenig, 2018) On the other hand, the temporal dynamics, the occurrence and the transitions between microstates are sensitive to the temporary brain state (Michel and Koenig, 2018; Khanna et al., 2014; Tomescu et al., 2018; da Cruz et al., 2020; Zanesco et al., 2021).

Given these premises, a comprehensive assessment of spatio-temporal brain dynamics in patients with pDoC via microstates analysis may lead to understanding which brain states are related to altered consciousness levels and to specific types of neurophysiological patterns. In the present work, we analyzed low-density, routinely collected EEG recordings of patients, extracting information on brain microstates. Such data was taken from a large, prospectively-collected, cohort of patients with a sABI enrolled in the PRABI study (Predictors of Recovery in patients with severe Acquired Brain Injuries) (Hakiki et al., 2022). We then studied microstates’ features, spatio-temporal dynamics and complexity across consciousness alterations and different neurophysiological conditions typical of sABI patients reported following international guidelines. Finally, the same features were used for prognostic analyses targeting the discharge consciousness state of a sub-cohort of patients with pDoC.

2. Materials and methods

2.1. Patients and clinical evaluation

A prospective observational study was performed enrolling consecutively patients admitted to IRCCS Fondazione Don Carlo Gnocchi of Florence from 10 to 06-2020 to 01–06-2022 (Hakiki et al., 2022). Inclusion criteria were diagnosis of a sABI, time post-onset < 4 months, age > 18, clinical stability. Approval from the local Ethical Committee was obtained (N. 16606_{OSS}) and enrolment was done following the Helsinki Declaration. Additional exclusion criteria were: i) absence of at least 5 clean minutes of resting-state EEG, ii) excessive movement artifacts, iii) detached channel during the recording, or iv) rejection of more than 3 channels according to the PREP criteria. (Bigdely-Shamlo et al., 2015) Patients have been included after obtaining a written consent signed by a legal guardian. Data concerning demographical and clinical aspects were recorded. Based on the highest value scored across at least five consecutive CRS-R evaluation with the best score retained for the analysis, a clinical diagnosis of consciousness was formulated both at admission and at discharge following international guidelines (Giacino et al., 2005; Wannez et al., 2017; Wang et al., 2020).

2.2. EEG recording and ACNS labelling

Standard clinical 30-minute EEG recordings were performed using a digital machine (Gal NT, EBNeuro). An EEG prewired head cap, with 19 electrodes (Fp1-Fp2-F7-F8-F3-F4-C3-C4-T3-T4-P3-P4-T5-T6-O1-O2-Fz-Cz-Pz) set according to the 10–20 International Standard System was adopted with previously proposed EEG recording parameters (Scarpino et al., 2019; Scarpino et al., 2020) at a sample rate of 128 Hz. Recordings were performed with closed eyes and included an initial 10-minutes part of resting-state and 20-minutes of randomly administered stimuli. The entire recording (resting state + stimuli) was only used to report the ACNS Critical Care terminology. In particular, EEG labelling was performed by the agreement of two expert neurologists (M.S., A.G.) according to the related guidelines (Hirsch et al., 2021). The included descriptors were frequency (delta or theta), voltage (normal or low), presence of an anterior/posterior gradient (APG) in the background activity, presence of a symmetric brain background and lastly, presence of reactivity. APG was labeled if at any point in the epoch, a clear and persistent (>1 continuous minute) anterior to posterior gradient of voltages and frequencies was present. In particular, lower amplitude and faster frequencies were seen in anterior derivations while higher amplitude and slower frequencies were seen in posterior derivations. An EEG recording was labeled as reactive if a change in background EEG activity (amplitude or frequency) was present upon stimulation. Reactivity could also be labeled as not constant when such change was not found repeatable across stimulations. Symmetry was defined as present when a consistent asymmetry in amplitude or in frequency was present for at least 50 % of the epochs.

2.3. EEG pre-processing

Only the resting state portion of the EEG was used for microstate extraction and thus entered the preprocessing step. Each recording was visually inspected for excessive movement noise and the patient was retained for further analysis if at least 5 consecutive minutes of clean resting-state EEG were present. The initial and endpoint of the 5-minutes section were manually taken and used to crop the recording (Fig. 1). Consequently, unipolar recordings were re-referenced to the grand average and high-pass filtered using the MNE library (Gramfort et al., 2013). In particular, a finite-impulse-response zero-phase filter with a Hamming's window was applied to band-pass only components between 1 and 30 Hz as suggested by the PREP pipeline (Bigdely-Shamlo et al., 2015). Infinite-impulse-response notch (50 Hz) filtering was then applied to further remove power line disturbance. Then, the first five seconds of the recording were discarded to eliminate filtering artifacts. Channels with still excessive or uncorrelated noise were labeled following PREP criteria (Bigdely-Shamlo et al., 2015) and interpolated by means of spherical spline interpolation (Perrin et al., 1989; Freeden, 1984) using the MNE library.

Lastly, the extended InfoMax Independent Component Analysis (ICA) method was applied to remove artifacts prior to signal reconstruction (Bell and Sejnowski, 1995). Within this step, a pre-whitening Principal Components Analysis (PCA) step was applied, decreasing dimensionality from $N_{channels}$ to $N_{components}$ with $N_{components} = 15$. The whitened data, then entered into the ICA algorithm. Independent components (ICs) were automatically labelled and excluded (confidence lower than 80 %) using the MNE-ICALabel library (Li et al., 2022) (a neural-network classifier trained on crowd-sourced data, based on the Matlab ICLabel implementation (Pion-Tonachini et al., 2019). Channel-level data was then reconstructed from the ICs spaces after including only brain data.

2.4. Microstate analysis

Patient-level microstate maps were estimated with a repeated clustering technique. For each K-channel EEG recording, the Global Field Power (GFP) was computed as the standard deviation across all electrodes at time t,

$$GFP(t) = \sqrt{\frac{\sum_K (V_i(t) - V_{mean}(t))^2}{K}}$$

with V_i being the potential of the i-th electrode and V_{mean} being the grand-average across all electrodes. The GFP peaks were detected and provided as input into a modified k-means algorithm. For each patient, the algorithm was executed 50 times and the solution minimizing the intra-cluster distance was retained for further analysis, in order to avoid falling into local minima. Such procedure was repeated with a variable number of clusters (from 3 to 10). For each patient the cross-validation

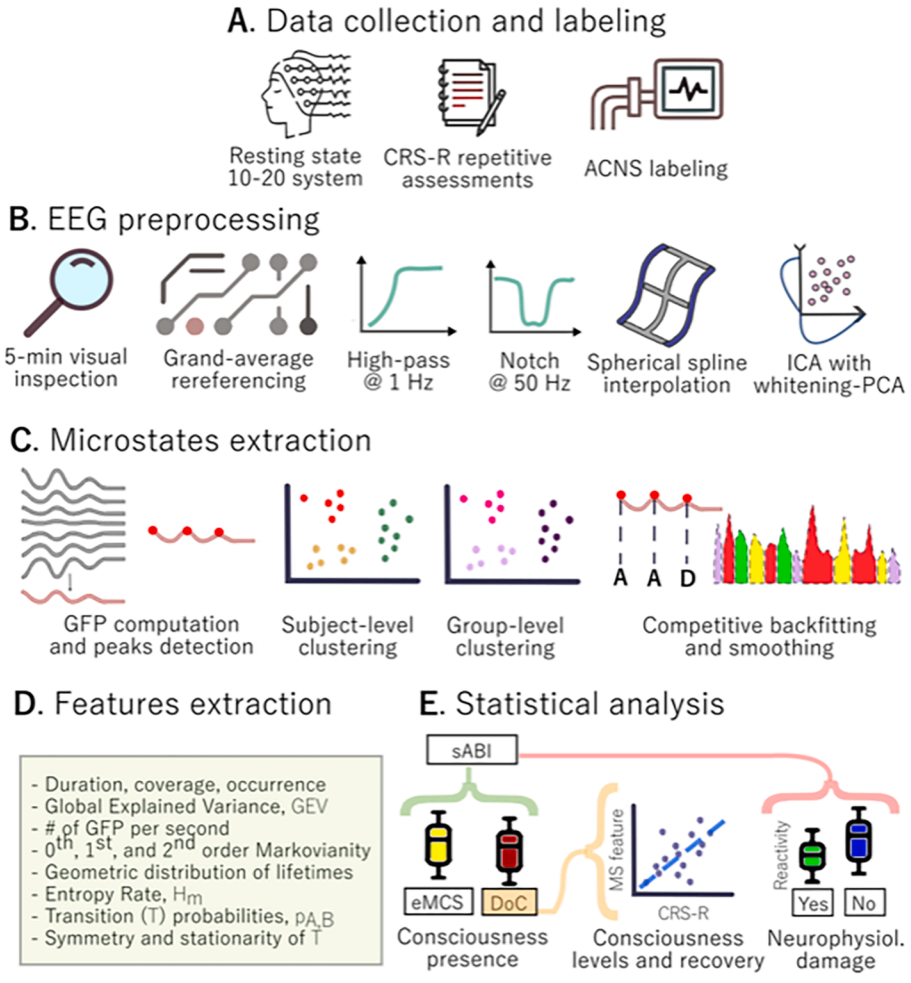

Fig. 1. Study pipeline. EEG recordings are collected and labelled together with consciousness assessments (**A**). Recordings are pre-processed to obtain an artifact-free recording (**B**) and then entered the microstates extraction step (**C**). After obtaining the backfitted microstate sequence, features related to either the sequence or the transition matrix is extracted (**D**). Patients' features entered different statistical analysis (**E**) targeting i) the presence/absence of a DoC, ii) different consciousness levels within the DoC sub-cohort and iii) different ACNS descriptors of the neurophysiological damage.

criterion (CV) as introduced by Pascual-Marqui et al., was computed. The average of patients' CV across number of clusters was taken and the optimal number of clusters was found by estimating the elbow point as in Satopa et al. on the CV-$N_{microstates}$ curve. Once retrieved the optimal $N_{microstates,}$ and the related microstate sequence, a second clustering step ($N_{iterations} = 500$) was applied to the individual topographies, to reduce patient-level variability in individual maps. The grand-average topographies were ordered following Michel and Koening (Michel and Koenig, 2018) and then backfitted onto the individual patients' GFP peaks with a winner-takes-all procedure. In particular, the microstate minimizing the Global Map Dissimilarity with the map at each time point *t*, was assigned to that timepoint.

Lastly, to reduce the likelihood of having abnormally small microstate activations, the backfitting process was smoothed. In particular, the group-maps assignment was done to iteratively avoid segments shorter than 30 ms, by assigning the label to the second best (i.e., competitive backfitting). In the end, for each patient a sequence of microstates π was derived and retained for feature extraction. The microstate extraction process was performed via the eeg-microstates library (von Wegner et al., 2018) and custom python code.

2.5. Microstate features

For each patient, the sequence of microstates π was used to extract the related features. For each microstate, the mean duration, occurrence and coverage were extracted. In particular, the duration of a microstate corresponds to the time interval that is assigned to that microstate, and the mean duration is average across all segments of that microstate. The occurrence represents the average number of appearances that a microstate makes within one second and the coverage is the fraction (of time) of the total recording length occupied by a microstate. Lastly, the percentage of total variance explained (of the whole π sequence) by a given microstate (Global Explained Variance, GEV) was computed (Brodbeck et al., 2012). The information content of the microstates' distribution was quantified by estimating the Shannon entropy *H* of the sequence as follows

$$H = -\sum\nolimits_{n} \mathrm{p(n)logp(n)}$$

with n running over the microstate labels, and $p(n)$ the probability of the microstate *n*. *H* is estimated in *nats*, thus using natural logarithm. Then, the entropy rate of the sequence (H_m) is estimated from a set of Shannon entropies *H* for varying history lengths m as the slope of the linear fit m versus H_m.

To test memory effects within the backfitted microstate sequence, the Markov properties of order 0, 1, and 2 were tested. For example, testing for 0-th order Markovian properties aims to evaluate whether

$$P\left(X_{t+1}|X_t\right) = P\left(X_{t+1}\right)$$

expanded up the order k = 2 as follows:

$$P\left(X_{t+1}|X_t, X_{t-1}, X_{t-(k-1)}, \cdots, X_{t-k}\right) = P\left(X_{t+1}|X_t, X_{t-(k-1)}\right)$$

To get a feeling of the temporal dynamics of the recording spatial variance, the number of GFP per second was also computed. Also, transition probabilities between all pairs of microstates labels were assessed via the 4x4 transition matrix $\widehat{T}$. Each $\widehat{T}$ was tested for symmetry and stationarity. The first evaluated whether each state transition occurred with the same probability of the opposite transition. This was performed by testing the following:

$$P(X_{t+1} = S_i|X_t = S_j) = P\left(X_{t+1} = S_j\middle|X_t = S_i\right)$$

with S_i, S_j two different states (e.g., A, B).

Stationarity of the transition matrix was the independence of the number of transitions between S_i and S_j (termed f_{ij}) within each block k (termed f_{ijk}) by the block index k. The hypothesis tested was the following

$$P\left(X_{t+1}^{(k)}|X_t^{(k)}\right) = P(X_{t+1}|X_t)$$

Lastly, first-order Markov surrogate chain was synthesized starting from the backfitted sequence following previous works (von Wegner et al., 2017; Häggström, 2002) and it was tested again for stationarity, asymmetry, and for geometric lifetime distribution of each microstate.

2.6. Statistical analysis

Microstates features were reported via median and interquartile ranges (when numerical) and via counts and percentages (when categorical, e.g., dichotomized p-values). A preliminary analysis on microstate features was done considering classes as repeated measures. Thus, features entered a Friedman ANOVA analysis and conditioned to its significance, pairwise FDR-corrected post-hoc analysis were carried out.

Individual class features (e.g., duration, GEV) and sequence related ones (e.g., entropy, GFP peaks per second) were compared among consciousness levels (eMCS, MCS+, MCS-, and UWS) entering Jonckheere-Terpstra test for ordered alternatives, and conditioned to significant group differences, post-hoc FDR corrected analysis were carried out.

Features which showed group differences, also entered a correlational analysis with the admission and discharge CRS-R value. This analysis was limited only to the pDoC population (UWS, MCS-, and MCS +). When evaluating prognostic power of the microstate features, linear regressions were adjusted by known confounding factors (i.e., age, sex, time post-onset, etiology, admission CRS-R, background frequency and reactivity, and APG), always correcting for FDR. Whenever the microstate features survived FDR correction, the corresponding full model was compared with the reduced model (without the microstate feature) via the Chow test, to compare model coefficients, and the variation of F-ANOVA between residuals, to understand whether microstate data significantly improved model performances (i.e., explained variance).

When performing analysis conditioned to the presence/absence of reactivity, patients labelled as unclear were excluded to avoid misassignment in one category, while patients with non-constant reactivity were combined with the ones with absent reactivity. Also, whenever the antero-posterior gradient (APG) was labeled unclear, the corresponding patient was removed from the APG-related analysis.

3. Results

3.1. Population

Out of the 415 patients enrolled in the study, 174 were excluded due the additional inclusion criteria on the EEG recordings. One hundred seventy-five patients were retained for microstate extraction. Of these 241, 14 were removed from the statistical analysis given missing data across clinical variables (i.e., aetiology, consciousness state).

The resulting 229 patients formed the analysed cohort (median age 66 years [IQR = 21], 89 females, 38.9 %, median time post-onset 38 days [IQR = 23], Table 1). The cohort resulted having a median CRS-R value of 20 points [IQR = 11] with 131 eMCS patients (CRS-R: 23 [IQR = 1], 26 MCS+ (CRS-R: 13 [IQR = 5]), 41 MCS- (CRS-R: 9 [IQR = 2]), and 31 UWS (CRS-R: 4 [IQR = 2]). The patients' aetiologies resulted distributed as follows: 68 patients with a traumatic brain injury, 13 anoxic, 42 ischemic, 98 haemorrhagic patients and 8 patients with other aetiology (tumoral, encephalitic, infectious or mixed).

ACNS Critical Care labelling resulted in 142 (62.0 %) patients having an θ background and 124 patients (54.1 %) with a symmetric brain activity (Table 1). The majority of the patients (N = 178, 85.2 %) were found to have an anteroposterior reorganization of brain activity (2′ patients had an APG labelled unclear). Reactivity was found to be present in 90 patients and absent (not-constant) in 118 patients (unclear in the remaining).

Table 1
Descriptive demographic and clinical data for the analysed cohort of sABI patients.

	Median [IQR] Count (%)
Age, *years*	66 [21]
Gender, *females*	89 (38.9)
TPO, *days*	38 [23]
Etiology	–
TBI	59 (25.8)
Anoxic	15 (6.6)
Ischemic	44 (19.2)
Hemorrhagic	101 (44.1)
Other	10 (4.3)
Consciousness State	
UWS	31 (13.5)
MCS-	26 (11.4)
MCS+	41 (17.9)
eMCS	131 (57.2)
CRS-R	20 [12]
Symmetry, *present*	124 (54.1)
Frequency, θ	142 (62.0)
APG, *present* (N = 209)	178 (85.2)
Reactivity, *present* (N = 208)	90 (43.3)

Legend. APG: Antero-Posterior Gradient CRS-R: Coma Recovery Scale-Revised; eMCS: emergence from MCS; MCS: Minimally Conscious State; TBI: Traumatic Brain Injury; TPO: Time Post-Onset; UWS: Unresponsive Wakefulness State.

3.2. Microstates: Estimation and distribution

Results of the cluster estimation and the related group-level microstate maps were reported in Fig. 2. The number of clusters with lowest CV criterion value (median across patients 0.49, Fig. 2A) was found to be three (median cumulative GEV of subject-level maps of 0.64, Fig. 2B). Group-level microstate maps were reported in Fig. 2C, ordered following Konig et al.

Coverage, duration, occurrence, and GEV of the backfitted group-level microstate sequence were found to be significantly different across classes ($p < 0.05$, Table 2).

In particular, coverage and occurrence of the A microstate were found to be significantly higher than the one of the B and C classes (all surviving FDR correction except A-C coverage comparison, Table 2, Fig. 3). GEV_C (median 0.150 [IQR = 0.145]) was found to be significantly higher than GEV_A (median 0.109 [IQR = 0.108], $p_{ADJ} = 0.003$) and GEV_B (median 0.112 [0.081], $p_{ADJ} = 0.001$).

3.3. Microstates: Consciousness diagnosis

Microstate features were then analyzed as individual classes. Class A duration (Fig. 4) was found to significantly be different across consciousness states ($p = 0.005$, $J = 6569.000$), with significantly higher duration ($p_{ADJ} < 0.05$) in the UWS patients (median 0.132 [IQR = 0.041]) than in eMCS patients (median 0.114 [IQR = 0.040]).

Similarly, class B duration (conditioned to group-level significant differences $p < 0.001$, $J = 5993.000$) was found to be significantly longer in UWS and MCS + patients compared to eMCS ones ($p_{ADJ} < 0.05$). Weakly significant was also the comparison between UWS and MCS- patients ($p_{ADJ} = 0.052$). Microstate C had a significantly difference coverage, occurrence and GEV across consciousness stated, however with only the eMCS-UWS GEV comparison surviving FDR correction ($p_{ADJ} < 0.05$).

Transition probabilities going from class A to C ($p_{A,C}$) and B to C ($P_{B,C}$) were found to be significantly higher at better consciousness levels ($p = 0.001$ and $p < 0.001$ respectively, Table 3). After post-hoc analysis, eMCS patients were found to have higher $P_{B,C}$ than MCS+ ($p = 0.001$), MCS- ($p = 0.046$), and UWS ($p = 0.001$) patients. Similarly, $P_{A,C}$ was significantly different in the eMCS-MCS + comparison ($p = 0.002$) and in the eMCS-UWS comparison ($p = 0.009$). Lastly, an higher entropy rate was found in eMCS patients compared to MCS+ ($p = 0.024$), MCS- ($p = 0.036$), and UWS ($p = 0.007$) patients, with only the eMCS-UWS comparison surviving FDR correction ($p_{ADJ} = 0.021$).

After selecting only, the pDoC cohort (UWS, MCS-, and MCS + patients), correlational analysis between CRS-R levels and microstate features, reported positive correlation ($R = 0.312$) between GEV_C and admission CRS-R score ($p = 0.002$, Table 4).

No significant differences between groups were found after testing the microstate sequences for 1st, 2nd, and 3rd Markovianity and each microstate lifetime for a geometric distribution ($p > 0.05$, Chi-Square analysis). Overall, most sequences were found to be significant at the 0th and 1st Markov order while less than 20 % of were found to be 2nd Markov order. Entropy estimates were confirmed by testing synthetic surrogate 1st order Markov Chains (Supplementary Table 2). Transition matrices were found to be symmetric in both groups (eMCS: 75, 93.8 %; pDoC: 85, 94.4 %) and mostly time-stationary (eMCS: 63.7 %, pDoC: 58.9 %), however none of the tests was significantly different between consciousness groups.

3.4. Microstates: Consciousness recovery

All microstate features were first univariately correlated with the CRS-R total score of the pDoC group at discharge from intensive rehabilitation (Table 4, centre column). A higher coverage ($p = 0.001$), occurrence ($p < 0.001$), and GEV ($p < 0.001$) of the C microstate were found to be correlated with higher CRS-R discharge values. Each of the significant variables in Table 4 entered a multivariate linear regression together with admission CRS-R, age, aetiology, time post-onset, frequency, reactivity, and APG (Table 4, right column).

In all the performed multivariate analysis, the admission CRS-R was found to be significant (positively correlated with discharge values) as well as the included microstate feature. Coverage ($\beta = 12.367$, 95 %CI: 3.550–21.184, $p = 0.007$), occurrence ($\beta = 11.066$, 95 %CI: 2.797–19.335, $p = 0.009$), and GEV (19.856, 95 %CI: 4.640–35.073, $p = 0.011$) of the C microstate were all found to be independent predictors of discharge CRS-R, with coverage also surviving FDR correction ($p_{ADJ} = 0.049$).

4. Discussions

The diagnosis and prognosis of patients with a pDoC is among the most challenging issues in the neurological sciences of the past two decades eliciting different clinical, economic and ethical questions (Farisco et al., 2022). In this context, identifying endotypes able to separate covert behavioural symptoms into stable sets of neurophysiological determinants has covered most of the research on consciousness. Current guidelines (Kondziella et al., 2020; Claassen et al., 2021) start from a behavioral assessment of consciousness, advocating for a secondary endotypical confirmation, often based on neuroimaging. Such necessity has been confirmed by overwhelming evidence that consciousness can occur in pDoC patients also in complete absence of intentional behaviour (Kondziella et al., 2020; Claassen et al., 2021) calling for a revision of its taxonomy (Bayne et al., 2017). Such revision has been performed using only neuroimaging-based, source-level derived information. In this optic, scalp-level data has often been discarded given the complexity of retrieving active/inactive sources and the well-known volume-conduction effect (van den Broek et al., 1998).

However, being able to identify endotypes sharing similar neurophysiological characteristics allows to identify the customized recovery paths. In doing this, it is mandatory to foster translatability to clinical practice of the technique within different levels of care providers and nation's wealth (Kondziella et al., 2021). In this work, we used EEG data collected during daily routine recordings in patients with a sABI (and in a pDoC) to understand whether scalp-level spatio-temporal dynamics could converge into specific endotypes of consciousness presence.

Currently, authors linked the four fundamental microstate dynamics with activity-specific neural patterns in healthy individuals. Microstates

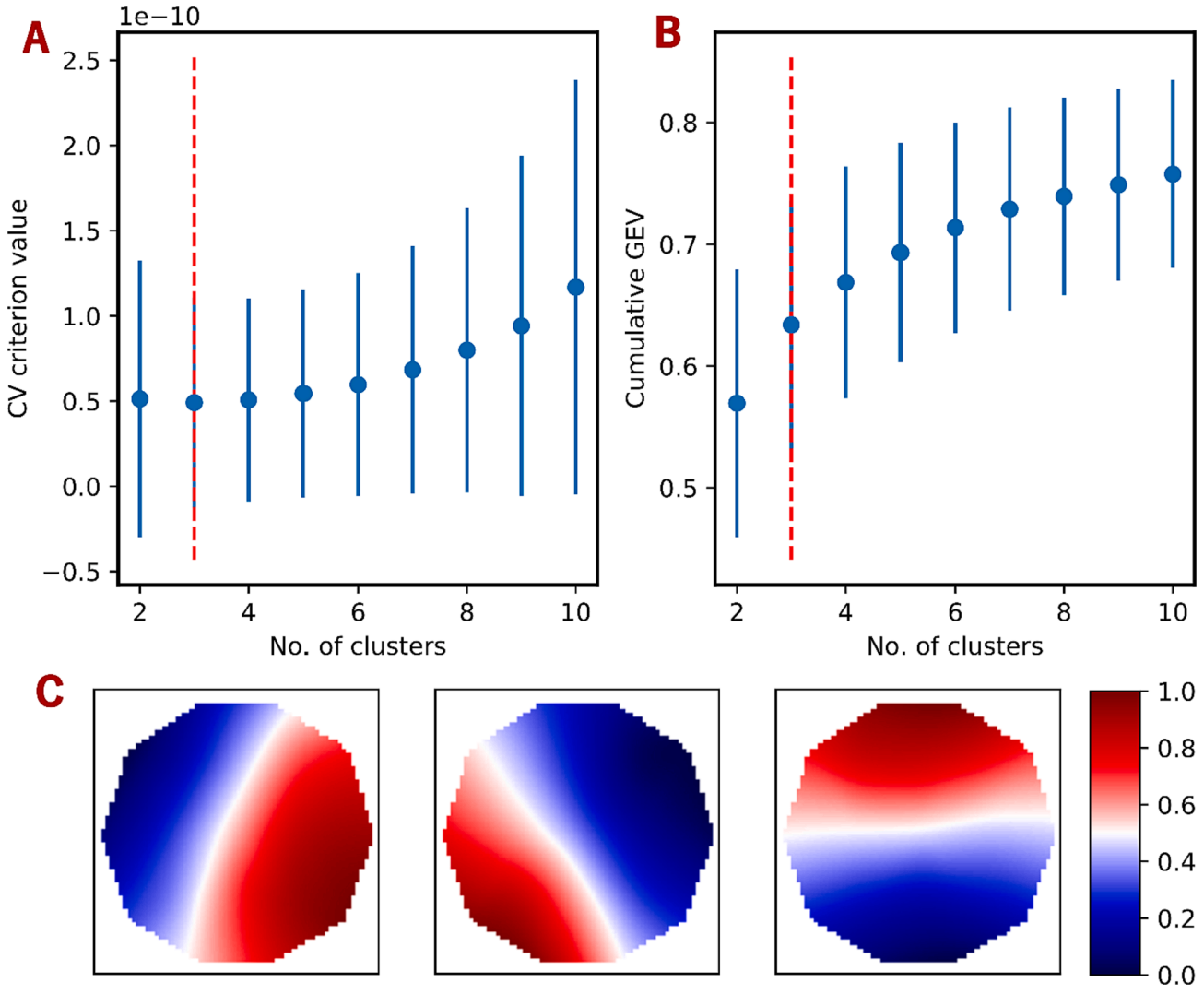

Fig. 2. Microstate maps. CV criterion value (A) and cumulative GEV (B, sum of GEV across all microstates) of all patients across different number of clusters. Dashed red line indicates the elbow-point, and thus the number of clusters used for further analysis. Blue dot (and line) indicate the mean (and standard deviation) across patients. In panel C, group-level microstate maps are reported, reordered according to visual similarity to Koenig et al., following the A, B, C syntax. (For interpretation of the references to colour in this figure legend, the reader is referred to the web version of this article.)

Table 2
Descriptive statistics and statistical comparison (median and interquartile range, in brackets) of the microstate features across classes. Friedman ANOVA was used for independent variables with more than two groups (e.g., coverage, GEV), while Wilcoxon Sum Rank test for paired samples was used for independent variables with two groups (e.g., transition probability due to the removal of the same-state persistence probability). P-values reported in the table are not FDR corrected.

	A	B	C	p-value	Test statistics	$p_{A,B}$	$p_{A,C}$	$p_{B,C}$
Coverage	0.361 [0.165]	0.305 [0.117]	0.305 [0.181]	**0.009**	9.459	**0.003**	**0.025**	0.483
Duration	0.117 [0.047]	0.112 [0.036]	0.118 [0.053]	**0.036**	6.664	**0.010**	0.283	0.135
Occurrence	0.351 [0.182]	0.293 [0.125]	0.297 [0.195]	**0.003**	11.897	**0.001**	**0.007**	0.607
GEV	0.109 [0.108]	0.112 [0.081]	0.150 [0.145]	**<0.001**	17.852	0.709	**<0.001**	**<0.001**
Transition from A	–	0.034 [0.018]	0.037 [0.023]	**0.035**	2.109	–	–	–
Transition from B	0.039 [0.021]	–	0.041 [0.022]	**0.039**	2.059	–	–	–
Transition from C	0.043 [0.025]	0.042 [0.024]	–	0.946	0.067	–	–	–

Legend. GEV: Global Explained Variance.

A and B were found to have a larger coverage during visualization and verbalization respectively (Milz et al., 2016). Somatic awareness (Pipinis et al., 2017) was found to be connected to frontal microstate dynamics, together with comfort and self-domain (Tarailis et al., 2021). On this matter, Giordano et al. speculated how microstates A and B may correspond to an extrinsic system while microstates C may correspond to an intrinsic system (Giordano et al., 2018). Also, prior studies demonstrated that all microstates' temporal dynamics are slowed down during drowsiness, anaesthesia or sleep (Bréchet and Michel, 2022; Brodbeck et al., 2012; Hao et al., 2022) and that as the microstate dynamics become slower, there is a smaller request for complex brain activity (Hao et al., 2022). However, it must be mentioned that, within healthy individuals the microstate C covers the majority of the GFP sequence (absolute and relative duration (Michel and Koenig, 2018; Hao

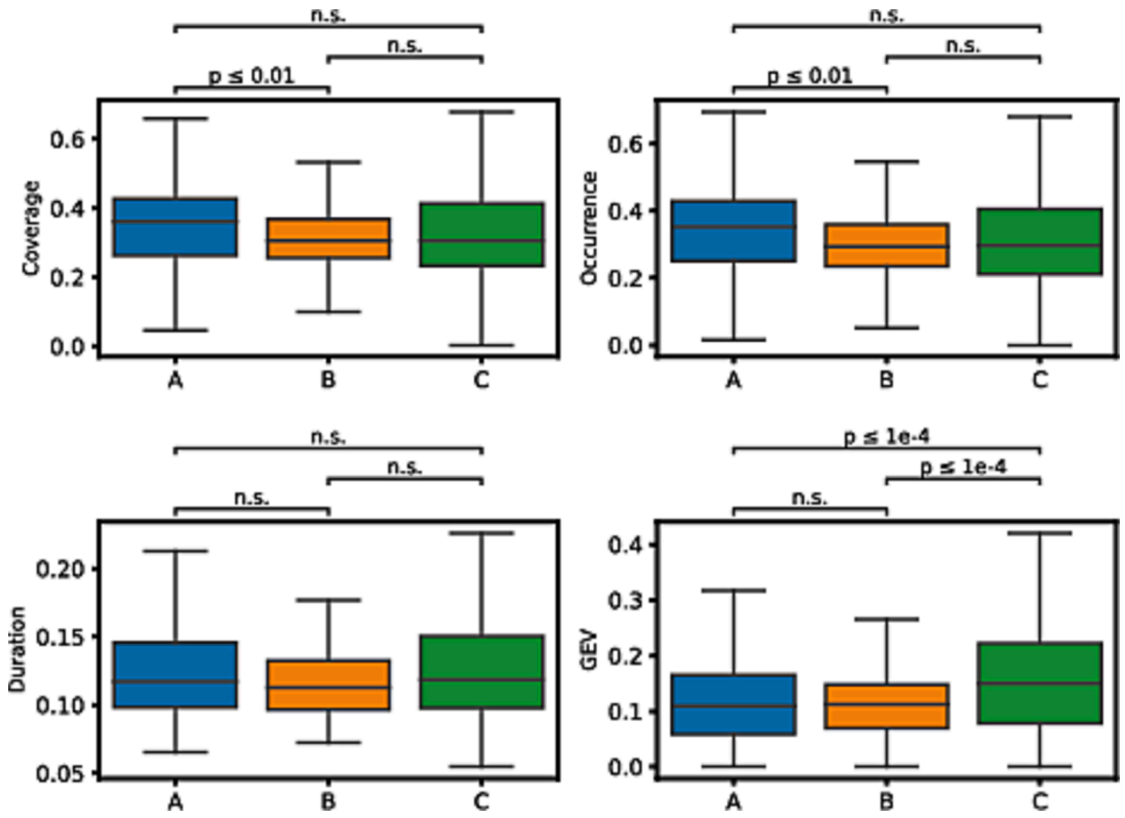

Fig. 3. Microstate descriptors. Coverage, occurrence, duration, and GEV of all microstates symbols with results of post-hoc FDR corrected tests in brackets.

et al., 2022; Artoni et al., 2022), independently from the EEG recording protocol (e.g., eyes-open, closed, anesthetized). Such persistent pattern of the microstate C was found to be almost disappearing in patients with a pDoC, contrarily to the substantial increase of the microstates A and B. Coherently, in our study we found how the GEV, coverage and duration of the C microstate is related to higher levels of consciousness, and to a better recovery from a pDoC state. Moreover, the relation between (un) consciousness and the absence of the C dynamics confirms a prior microstate analysis of fMRI data; anterior maps were found to be significantly more occurrent in MCS patients than in UWS (Zhang et al., 2023) as well as the transition from the sensorimotor state (extrinsic system, A-B maps) to an anterior (intrinsic system, C map) one. Further evidence in favour of our findings derives from the mutual dependence of awareness (perceptual) and microstate dynamics found by Britz et al. (Britz et al., 2014). Precisely, the group template of an aware pre-stimulus microstate was found to be fully anterior compared to the almost vertically symmetric one of (Fig. 4A/B of Britz et al.) an unaware one. Croce et al. reported how rTMS-based inhibition of specific areas changes only the topography of the C microstate, with no significant differences in the other three common templates (Croce et al., 2018). Furthermore, the C map was affected by rTMS whenever the stimulation site belonged either in the Dorsal Attention Network (DAN, i.e., left and the right Intra-Parietal Sulcus) or in the Default Mode Network (DMN, i. e., left and right Angular Gyrus). C map was not affected whenever the stimulation occurred in the Temporo-Parietal Junction (TPJ), coherent with the fact that TPJ does not belong to either the DAN or DMN.

Lastly, temporal dynamics of the C microstate in persons with multiple sclerosis did not differ with healthy individuals, showing how neurological disorders without consciousness alterations do not affect this specific brain state. However, during propofol-induced consciousness alterations, individuals in a moderate sedation resulted having a significantly lower coverage of the C microstate (Liu et al., 2022), showing how in patients with no structural connectivity damages, but *temporary* consciousness alterations, the distribution of frontal microstates is affected. All the aforementioned evidence allows us to speculate that the ability of the brain of persisting in (transitioning to) the C state is a sine qua non of consciousness, besides being related to the precuneus/posterior cingulate cortex DMN activations. (Fransson and Marrelec, 2008) However, the presence of the C microstate, even if characterized by low coverage/duration, can occur while consciousness is absent, thus microstates may be necessary to sustain consciousness, but cannot be considered as the only actor in consciousness presence/recovery. In general, the microstates description of the brain temporal dynamics by consecutive global perceptual frames yields a microstate syntax, which is self-similar (i.e., exhibits the same behaviour at different timescales). Viewing such self-similarity as an internal clock (i. e., responsible for synchronizing subsequent brain dynamics) and consciousness as composed by elementary building block of cognition (i.e., microstates), perfectly fits the Higher-Order Theories (HOTs) and the Global Workspace Theories (GWTs) of consciousness. The first postulates the dependence of consciousness from latent representations of lower-order brain states (e.g., microstates), with the anterior cortex (namely prefrontal cortex) the main site involved in performing higher-order representations. The second, GWTs propose the division of the brain into critically specialized sub-modules connected via short- and long- range links, with the fronto-parietal region being the focal point. Contextualizing our findings within such frameworks puts another foot toward an *anteriorization* of consciousness. In particular, for consciousness to occur, the brain must be able to sustain a persistent antero-posterior dynamic (C microstate), while for consciousness to recover, the L-R microstates must decrease in favor of A-P ones.

Surely, further investigations would exclude the possibility that different maps in different patient groups arose from a difference in brain injury. Indeed, this is a current limitation of this work given that structural MRI scans were not collected together with the EEG recordings. Furthermore, the "winner-take-all" strategy adopted to assign microstate labels does not take into account the possibility of existing competing microstates, hypothesizing a discontinuous EEG evolution. In

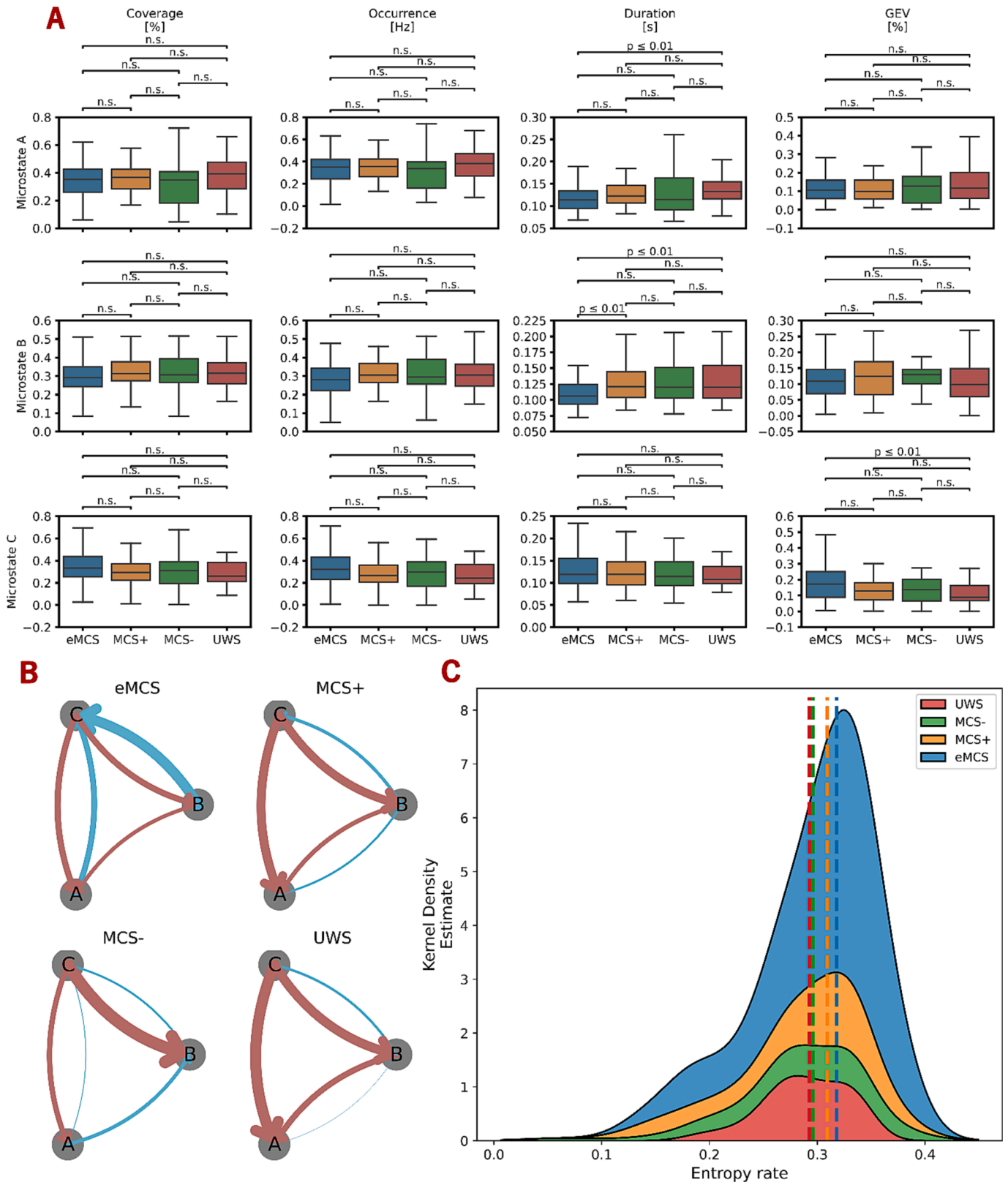

Fig. 4. Microstate and consciousness presence. Microstates' coverage, duration, occurrence, and GEV compared between consciousness levels with results of post-hoc FDR corrected tests in brackets (panel A). Transition probabilities between classes (panel B) and the entropy rate of the microstate sequence (panel C) are reported for each consciousness levels. In panel C, dashed lines indicate the mean entropy rate of the group. **Legend**. UWS: Unresponsive Wakefulness State; MCS: Minimally Conscious State; eMCS: emergence from MCS; GEV: Global Explained Variance.

Table 3
Median and interquartile ranges (in brackets) for microstate classes and sequence features and results of the statistical comparison among consciousness states (Jonckheere-Terpstra test for ordered alternatives).

	eMCS	MCS+	MCS-	UWS	p-value	Test statistics
Coverage						
A	0.351 [0.167]	0.365 [0.142]	0.348 [0.238]	0.392 [0.202]	0.281	7431.000
B	0.292 [0.111]	0.312 [0.107]	0.307 [0.163]	0.315 [0.119]	**0.030**	6867.500
C	0.332 [0.187]	0.294 [0.171]	0.311 [0.223]	0.259 [0.175]	**0.009**	9339.000
Duration						
A	0.114 [0.040]	0.122 [0.043]	0.115 [0.092]	0.132 [0.041]	**0.006**	6569.000
B	0.106 [0.354]	0.121 [0.219]	0.119 [0.053]	0.120 [0.058]	**<0.001**	5993.000
C	0.119 [0.058]	0.119 [0.055]	0.114 [0.060]	0.107 [0.039]	0.351	8474.000
Occurrence						
A	0.351 [0.178]	0.355 [0.160]	0.335 [0.250]	0.382 [0.219]	0.314	7468.500
B	0.281 [0.125]	0.304 [0.109]	0.295 [0.159]	0.304 [0.125]	**0.044**	6945.000
C	0.320 [0.199]	0.265 [0.168]	0.296 [0.248]	0.242 [0.172]	**0.008**	9361.000
GEV						
A	0.106 [0.100]	0.099 [0.104]	0.128 [0.155]	0.117 [0.145]	0.463	7610.000
B	0.108 [0.079]	0.124 [0.105]	0.130 [0.056]	0.098 [0.091]	0.532	7666.000
C	0.173 [0.163]	1.292 [0.113]	0.137 [0.137]	0.088 [1.055]	**<0.001**	9802.000
P_A						
to B	0.035 [0.017]	0.034 [0.018]	0.039 [0.023]	0.030 [0.015]	0.514	8329.000
to C	0.040 [0.025]	0.033 [0.016]	0.039 [0.029]	0.034 [0.023]	**0.001**	9674.000
P_B						
to A	0.039 [0.020]	0.036 [0.019]	0.033 [0.026]	0.039 [0.026]	0.199	8657.000
to C	0.046 [0.027]	0.037 [0.020]	0.041 [0.032]	0.035 [0.017]	**<0.001**	10053.000
P_C						
to A	0.043 [0.142]	0.042 [0.018]	0.039 [0.035]	0.052 [0.029]	0.647	7753.000
to B	0.042 [0.113]	0.042 [0.027]	0.048 [0.025]	0.042 [0.016]	0.748	7824.000
GFP peaks per *s*	34.754 [7.665]	33.09 [10.90]	37.100 [6.623]	34.843 [5.329]	0.482	7626.000
Entropy rate	0.318 [0.065]	0.309 [0.078]	0.296 [0.100]	0.292 [0.057]	**0.003**	9542.000

Legend. GEV: Global Explained Variance; P_X: transition probability from the microstate X to another microstate.

Table 4
R values (p-values in parenthesis) of Spearman's test between microstate features and admission (first column) and discharge (second column) CRS-R values. Within the third column, the standardized β (p-value in parenthesis) of a multivariate linear regression with discharge CRS-R adjusted for age, etiology, TPO, CRS-R in admission, background frequency, reactivity and APG. Correlations are computed only on the pDoC group (N = 98) and for the features significantly differing among consciousness levels.

	$CRS\text{-}R_{admission}$	$CRS\text{-}R_{discharge}$	$CRS\text{-}R_{discharge,\ MV}$
Coverage *B*	−0.030 (0.770)	−0.117 (0.263)	–
Coverage *C*	0.188 (0.063)	0.379 (**0.001**)	0.274 (**0.007**)
Duration *A*	−0.132 (0.195)	−0.089 (0.396)	–
Duration *B*	−0.013 (0.900)	0.061 (0.562)	–
Occurrence *B*	−0.026 (0.802)	−0.108 (0.301)	–
Occurrence *C*	0.175 (0.085)	0.369 (**<0.001**)	0.260 (**0.009**)
GEV *C*	0.312 (**0.002**)	0.420 (**<0.001**)	0.289 (**0.011**)
$P_{A\text{-}C}$	0.074 (0.469)	0.192 (0.063)	–
$P_{B\text{-}C}$	0.107 (0.296)	0.184 (0.076)	–
Entropy rate	0.052 (0.611)	−0.013 (0.901)	–

Legend. GEV: Global Explained Variance; TPO: Time Post-Onset; APG: AnteroPosterior Gradient.

conclusion, our work reveals how global brain dynamics, interpreted in the microstate's framework, shape and define some of the necessary conditions for consciousness presence, and thus a prognosis of its recovery. Given the importance of the conclusion derived, it should be considered to include these non-behavioral, instrumentally-based estimates of residual signs of consciousness within the clinical assessment of sABI patients, in particular for the diagnosis and prognosis of patients with a pDoC.

Funding

The study was funded by the Italian Ministry of Health under the "Ricerca Corrente RC2020-22 programs" and the 5xMille funds AF2018: "Data Science in Rehabilitation Medicine", AF2019: "Study and development of biomedical data science and machine learning methods to support the appropriateness and the decision-making process in rehabilitation medicine". The study was also funded by Regione Toscana (Bando Ricerca Salute 2018), TUNE-BEAM project (H14I20000300002) and by the Italian neuroscience and neurorehabilitation research hospitals network ("Rete IRCCS delle Neuroscienze e della Neuroriabilitazione").

Declaration of competing interest

The authors declare that they have no known competing financial interests or personal relationships that could have appeared to influence the work reported in this paper.

Data availability

All data needed to reproduce results presented within this manuscript are provided as a Supplementary file. Raw recordings can also be provided upon request for research and replication purposes only.

Appendix A. Supplementary data

Supplementary data to this article can be found online at https://doi.org/10.1016/j.nicl.2023.103540.

References

Alkhachroum, A., Eliseyev, A., Der-Nigoghossian, C.A., et al., 2020. EEG to detect early recovery of consciousness in amantadine-treated acute brain injury patients. J. Neurol. Neurosurg. Psychiatry 91 (6), 675–676. https://doi.org/10.1136/jnnp-2019-322645.

Artoni, F., Maillard, J., Britz, J., et al., 2022. EEG microstate dynamics indicate a U-shaped path to propofol-induced loss of consciousness. Neuroimage 256, 119156. https://doi.org/10.1016/j.neuroimage.2022.119156.

Aubinet C, Cassol H, Gosseries O, et al. Brain metabolism but not gray matter volume underlies the presence of language function in the minimally conscious state (MCS): MCS+ Versus MCS− Neuroimaging Differences. Neurorehabil Neural Repair. 2020; 34:154596831989991. 10.1177/1545968319899914.

Aubinet, C., Panda, R., Larroque, S., et al., 2019. Reappearance of command-following is associated with the recovery of language and internal-awareness networks: a

longitudinal multiple-case report. Front. Syst. Neurosci. 13. https://doi.org/10.3389/fnsys.2019.00008.
Bayne, T., Hohwy, J., Owen, A.M., 2017. Reforming the taxonomy in disorders of consciousness. Ann. Neurol. 82 (6), 866–872. https://doi.org/10.1002/ana.25088.
Bell, A.J., Sejnowski, T.J., 1995. An information-maximization approach to blind separation and blind deconvolution. Neural Comput. 7 (6), 1129–1159. https://doi.org/10.1162/neco.1995.7.6.1129.
Bigdely-Shamlo N, Mullen T, Kothe C, Su KM, Robbins KA. The PREP pipeline: standardized preprocessing for large-scale EEG analysis. Front Neuroinformatics. 2015;9. Accessed December 20, 2022. https://www.frontiersin.org/articles/10.3389/fninf.2015.00016.
Boly, M., Phillips, C., Balteau, E., et al., 2008. Consciousness and cerebral baseline activity fluctuations. Hum. Brain Mapp. 29 (7), 868–874. https://doi.org/10.1002/hbm.20602.
Boly, M., Garrido, M.I., Gosseries, O., et al., 2011. Preserved feedforward but impaired top-down processes in the vegetative state. Science 332 (6031), 858–862. https://doi.org/10.1126/science.1202043.
Bréchet, L., Michel, C.M., 2022. EEG microstates in altered states of consciousness. Front. Psychol. 13, 856697 https://doi.org/10.3389/fpsyg.2022.856697.
Bressler, S.L., 1995. Large-scale cortical networks and cognition. Brain Res. Brain Res. Rev. 20 (3), 288–304. https://doi.org/10.1016/0165-0173(94)00016-i.
Britz J, Díaz Hernàndez L, Ro T, Michel CM. EEG-microstate dependent emergence of perceptual awareness. Front Behav Neurosci. 2014;8. Accessed January 26, 2023. https://www.frontiersin.org/articles/10.3389/fnbeh.2014.00163.
Brodbeck, V., Kuhn, A., von Wegner, F., et al., 2012. EEG microstates of wakefulness and NREM sleep. Neuroimage 62 (3), 2129–2139. https://doi.org/10.1016/j.neuroimage.2012.05.060.
Chennu, S., Finoia, P., Kamau, E., et al., 2014. Spectral signatures of reorganised brain networks in disorders of consciousness. PLoS Comput. Biol. 10. https://doi.org/10.1371/journal.pcbi.1003887.
Chennu, S., Annen, J., Wannez, S., et al., 2017. Brain networks predict metabolism, diagnosis and prognosis at the bedside in disorders of consciousness. Brain J. Neurol. 140. https://doi.org/10.1093/brain/awx163.
Claassen, J., Akbari, Y., Alexander, S., et al., 2021. Proceedings of the first curing coma campaign NIH symposium: challenging the future of research for coma and disorders of consciousness. Neurocrit. Care 35 (Suppl 1), 4–23. https://doi.org/10.1007/s12028-021-01260-x.
Comanducci, A., Boly, M., Claassen, J., et al., 2020. Clinical and advanced neurophysiology in the prognostic and diagnostic evaluation of disorders of consciousness: review of an IFCN-endorsed expert group. Clin. Neurophysiol. 131 (11), 2736–2765. https://doi.org/10.1016/j.clinph.2020.07.015.
Croce, P., Zappasodi, F., Capotosto, P., 2018. Offline stimulation of human parietal cortex differently affects resting EEG microstates. Sci. Rep. 8 (1), 1287. https://doi.org/10.1038/s41598-018-19698-z.
da Cruz, J.R., Favrod, O., Roinishvili, M., et al., 2020. EEG microstates are a candidate endophenotype for schizophrenia. Nat. Commun. 11 (1), 3089. https://doi.org/10.1038/s41467-020-16914-1.
Deco, G., Jirsa, V.K., McIntosh, A.R., 2011. Emerging concepts for the dynamical organization of resting-state activity in the brain. Nat. Rev. Neurosci. 12 (1), 43–56. https://doi.org/10.1038/nrn2961.
Demertzi, A., Antonopoulos, G., Heine, L., et al., 2015. Intrinsic functional connectivity differentiates minimally conscious from unresponsive patients. Brain J. Neurol. 138. https://doi.org/10.1093/brain/awv169.
Dipasquale O, Cercignani M. Network functional connectivity and whole-brain functional connectomics to investigate cognitive decline in neurodegenerative conditions. Funct Neurol. 2017;31(4):191-203. 10.11138/FNeur/2016.31.4.191.
Edlow, B., Claassen, J., Schiff, N., Greer, D., 2020. Recovery from disorders of consciousness: mechanisms, prognosis and emerging therapies. Nat. Rev. Neurol. 17. https://doi.org/10.1038/s41582-020-00428-x.
Efron, R., 1970. The minimum duration of a perception. Neuropsychologia 8 (1), 57–63. https://doi.org/10.1016/0028-3932(70)90025-4.
Estraneo, A., Masotta, O., Bartolo, M., et al., 2020. Multi-center study on overall clinical complexity of patients with prolonged disorders of consciousness of different etiologies. Brain Inj. 35, 1–7. https://doi.org/10.1080/02699052.2020.1861652.
Farisco, M., Pennartz, C., Annen, J., Cecconi, B., Evers, K., 2022. Indicators and criteria of consciousness: ethical implications for the care of behaviourally unresponsive patients. BMC Med. Ethics 23 (1), 30. https://doi.org/10.1186/s12910-022-00770-3.
Fischer, C., Luaute, J., Morlet, D., 2010. Event-related potentials (MMN and novelty P3) in permanent vegetative or minimally conscious states. Clin. Neurophysiol. Off. J. Int. Fed. Clin. Neurophysiol. 121 (7), 1032–1042. https://doi.org/10.1016/j.clinph.2010.02.005.
Forgacs, P.B., Conte, M.M., Fridman, E.A., Voss, H.U., Victor, J.D., Schiff, N.D., 2015. A proposed role for routine EEGs in patients with consciousness disorders. Ann. Neurol. 77 (1), 185–186. https://doi.org/10.1002/ana.24311.
Forgacs, P.B., Frey, H., Velazquez, A., et al., 2017. Dynamic regimes of neocortical activity linked to corticothalamic integrity correlate with outcomes in acute anoxic brain injury after cardiac arrest. Ann. Clin. Transl. Neurol. 4 (2), 119–129. https://doi.org/10.1002/acn3.385.
Forgacs, P.B., Allen, B.B., Wu, X., et al., 2022. Corticothalamic connectivity in aneurysmal subarachnoid hemorrhage: relationship with disordered consciousness and clinical outcomes. Neurocrit. Care 36 (3), 760–771. https://doi.org/10.1007/s12028-021-01354-6.
Fransson, P., Marrelec, G., 2008. The precuneus/posterior cingulate cortex plays a pivotal role in the default mode network: evidence from a partial correlation network analysis. Neuroimage 42 (3), 1178–1184. https://doi.org/10.1016/j.neuroimage.2008.05.059.
Freeden, W., 1984. Spherical spline interpolation—basic theory and computational aspects. J. Comput. Appl. Math. 11 (3), 367–375. https://doi.org/10.1016/0377-0427(84)90011-6.
Giacino, J.T., Ashwal, S., Childs, N., et al., 2002. The minimally conscious state: definition and diagnostic criteria. Neurology 58 (3), 349–353. https://doi.org/10.1212/wnl.58.3.349.
Giacino, J., Kalmar, K., Whyte, J., 2005. The JFK coma recovery scale-revised: measurement characteristics and diagnostic utility. Arch. Phys. Med. Rehabil. 85, 2020–2029. https://doi.org/10.1016/j.apmr.2004.02.033.
Giacino, J., Fins, J., Laureys, S., Schiff, N., 2014. Disorders of consciousness after acquired brain injury: the state of the science. Nat. Rev. Neurol. 10. https://doi.org/10.1038/nrneurol.2013.279.
Giordano, G.M., Koenig, T., Mucci, A., et al., 2018. Neurophysiological correlates of Avolition-apathy in schizophrenia: a resting-EEG microstates study. NeuroImage Clin. 20, 627–636. https://doi.org/10.1016/j.nicl.2018.08.031.
Gramfort, A., Luessi, M., Larson, E., et al., 2013. MEG and EEG data analysis with MNE-python. Front. Neurosci. 7, 267. https://doi.org/10.3389/fnins.2013.00267.
Häggström O. Finite markov chains and algorithmic applications. Cambridge University Press; 2002. 10.1017/CBO9780511613586.
Hakiki, B., Donnini, I., Romoli, A., et al., 2022. Clinical, neurophysiological, and genetic predictors of recovery in patients with severe acquired brain injuries (PRABI): a study protocol for a longitudinal observational study. Front. Neurol. 13 https://doi.org/10.3389/fneur.2022.711312.
Hao Z, Xia X, Bai Y, Wang Y, Dou W. EEG Evidence reveals zolpidem-related alterations and prognostic value in disorders of consciousness. Front Neurosci. 2022;16. Accessed January 19, 2023. https://www.frontiersin.org/articles/10.3389/fnins.2022.863016.
Haveman, M.E., Van Putten, M.J.A.M., Hom, H.W., Eertman-Meyer, C.J., Beishuizen, A., Tjepkema-Cloostermans, M.C., 2019. Predicting outcome in patients with moderate to severe traumatic brain injury using electroencephalography. Crit. Care Lond. Engl. 23 (1), 401. https://doi.org/10.1186/s13054-019-2656-6.
Hirsch, L., Fong, M., Leitinger, M., et al., 2021. American clinical neurophysiology society's standardized critical care EEG terminology: 2021 Version. J. Clin. Neurophysiol. 38, 1–29. https://doi.org/10.1097/WNP.0000000000000806.
Hirschberg, R., Giacino, J.T., 2011. The vegetative and minimally conscious states: diagnosis, prognosis and treatment. Neurol. Clin. 29 (4), 773–786. https://doi.org/10.1016/j.ncl.2011.07.009.
Khanna, A., Pascual-Leone, A., Farzan, F., 2014. Reliability of resting-state microstate features in electroencephalography. PLoS One 9 (12), e114163.
King, J.R., Sitt, J., Faugeras, F., et al., 2013. Information sharing in the brain indexes consciousness in noncommunicative patients. Curr. Biol. CB. 23. https://doi.org/10.1016/j.cub.2013.07.075.
Koenig, T., Prichep, L., Lehmann, D., et al., 2002. Millisecond by millisecond, year by year: normative EEG microstates and developmental stages. Neuroimage 16 (1), 41–48. https://doi.org/10.1006/nimg.2002.1070.
Kondziella, D., Bender, A., Diserens, K., et al., 2020. European academy of neurology guideline on the diagnosis of coma and other disorders of consciousness. Eur. J. Neurol. 27. https://doi.org/10.1111/ene.14151.
Kondziella, D., Menon, D.K., Helbok, R., et al., 2021. A precision medicine framework for classifying patients with disorders of consciousness: advanced classification of consciousness endotypes (ACCESS). Neurocrit. Care 35 (Suppl 1), 27–36. https://doi.org/10.1007/s12028-021-01246-9.
Kotchoubey, B., 2005. Event-related potential measures of consciousness: two equations with three unknowns. Prog. Brain Res. 150, 427–444. https://doi.org/10.1016/S0079-6123(05)50030-X.
Kotchoubey, B., Lang, S., Mezger, G., et al., 2005. Information processing in severe disorders of consciousness: Vegetative state and minimally conscious state. Clin. Neurophysiol. 116 (10), 2441–2453. https://doi.org/10.1016/j.clinph.2005.03.028.
Lehmann, D., Faber, P.L., Galderisi, S., et al., 2005. EEG microstate duration and syntax in acute, medication-naive, first-episode schizophrenia: a multi-center study. Psychiatry Res. 138 (2), 141–156. https://doi.org/10.1016/j.pscychresns.2004.05.007.
Lehmann D. Brain electric microstates and cognition: the atoms of thought. In: John ER, Harmony T, Prichep LS, Valdés-Sosa M, Valdés-Sosa PA, eds. Machinery of the Mind: Data, Theory, and Speculations About Higher Brain Function. Birkhäuser; 1990:209-224. 10.1007/978-1-4757-1083-0_10.
Lehmann D. Brain electric microstates, and cognitive and perceptual modes. In: Kruse P, Stadler M, eds. Ambiguity in Mind and Nature. Springer Series in Synergetics. Springer; 1995:407-420. 10.1007/978-3-642-78411-8_20.
Leon-Carrion, J., Martin-Rodriguez, J.F., Damas-Lopez, J., 2009. Delta-alpha ratio correlates with level of recovery after neurorehabilitation in patients with acquired brain injury. Clin. Neurophysiol. Off. J. Int. Fed. Clin. Neurophysiol. 120 (6), 1039–1045. https://doi.org/10.1016/j.clinph.2009.01.021.
Li A, Feitelberg J, Saini A, Höchenberger R, Scheltienne M. MNE-ICALabel: Automatically annotating ICA components with ICLabel in Python. J Open Source Softw. 2022;7:4484. 10.21105/joss.04484.
Liu, Z., Si, L., Xu, W., et al., 2022. Characteristics of EEG microstate sequences during propofol-induced alterations of brain consciousness states. IEEE Trans. Neural Syst. Rehabil. Eng. 30, 1631–1641. https://doi.org/10.1109/TNSRE.2022.3182705.
Liuzzi, P., Magliacano, A., De Bellis, F., Estraneo, A., Mannini, A., 2022. Predicting outcome of patients with prolonged disorders of consciousness using machine learning models based on medical complexity. Sci. Rep. 12 (1) https://doi.org/10.1038/s41598-022-17561-w.

Liuzzi, P., Grippo, A., Campagnini, S., et al., 2022. Merging clinical and EEG biomarkers in an elastic-net regression for disorder of consciousness prognosis prediction. IEEE Trans. Neural Syst. Rehabil. Eng. 30, 1504–1513. https://doi.org/10.1109/TNSRE.2022.3178801.

Masson, F., Thicoipe, M., Aye, P., et al., 2001. Epidemiology of severe brain injuries: a prospective population-based study. J. Trauma 51 (3), 481–489. https://doi.org/10.1097/00005373-200109000-00010.

Michel, C.M., Koenig, T., 2018. EEG microstates as a tool for studying the temporal dynamics of whole-brain neuronal networks: a review. Neuroimage 180, 577–593. https://doi.org/10.1016/j.neuroimage.2017.11.062.

Milz, P., Faber, P.L., Lehmann, D., Koenig, T., Kochi, K., Pascual-Marqui, R.D., 2016. The functional significance of EEG microstates–associations with modalities of thinking. Neuroimage 125, 643–656. https://doi.org/10.1016/j.neuroimage.2015.08.023.

Panda R, López-González A, Gilson M, et al. Posterior integration and thalamo-frontotemporal broadcasting are impaired in disorders of consciousness. Published online July 5, 2022:2021.11.08.467694. 10.1101/2021.11.08.467694.

Perrin, F., Pernier, J., Bertrand, O., Echallier, J.F., 1989. Spherical splines for scalp potential and current density mapping. Electroencephalogr. Clin. Neurophysiol. 72 (2), 184–187. https://doi.org/10.1016/0013-4694(89)90180-6.

Pion-Tonachini, L., Kreutz-Delgado, K., Makeig, S., 2019. ICLabel: an automated electroencephalographic independent component classifier, dataset, and website. Neuroimage 198, 181–197. https://doi.org/10.1016/j.neuroimage.2019.05.026.

Pipinis, E., Melynyte, S., Koenig, T., et al., 2017. Association between resting-state microstates and ratings on the amsterdam resting-state questionnaire. Brain Topogr. 30 (2), 245–248. https://doi.org/10.1007/s10548-016-0522-2.

Rizkallah, J., Annen, J., Modolo, J., et al., 2019. Decreased integration of EEG source-space networks in disorders of consciousness. NeuroImage Clin. 23, 101841 https://doi.org/10.1016/j.nicl.2019.101841.

Scarpino, M., Lolli, F., Hakiki, B., et al., 2019. Prognostic value of post-acute EEG in severe disorders of consciousness, using american clinical neurophysiology society terminology. Neurophysiol. Clin. 49. https://doi.org/10.1016/j.neucli.2019.07.001.

Scarpino, M., Lolli, F., Hakiki, B., et al., 2020. EEG and coma recovery scale-revised prediction of neurological outcome in disorder of consciousness patients. Acta Neurol. Scand. 142 https://doi.org/10.1111/ane.13247.

Schiff, N.D., 2010. Recovery of consciousness after brain injury: a mesocircuit hypothesis. Trends Neurosci. 33 (1), 1–9. https://doi.org/10.1016/j.tins.2009.11.002.

Schiff, N.D., Mesocircuit Mechanisms Underlying Recovery of Consciousness Following Severe Brain Injuries: Model and Predictions. In: Monti MM, Sannita WG, eds. Brain Function and Responsiveness in Disorders of Consciousness. Springer International Publishing; 2016:195-204. 10.1007/978-3-319-21425-2_15.

Sitt, J., King, J.R., El Karoui, I., et al., 2014. Large scale screening of neural signatures of consciousness in patients in a vegetative or minimally conscious state. Brain J. Neurol. 137. https://doi.org/10.1093/brain/awu141.

Tarailis, P., Šimkutė, D., Koenig, T., Griškova-Bulanova, I., 2021. Relationship between spatiotemporal dynamics of the brain at rest and self-reported spontaneous thoughts: an EEG microstate approach. J Pers Med. 11 (11), 1216. https://doi.org/10.3390/jpm11111216.

Thibaut, A., Panda, R., Annen, J., et al., 2021. Preservation of brain activity in unresponsive patients identifies MCS star. Ann. Neurol. 90 (1), 89–100. https://doi.org/10.1002/ana.26095.

Tomescu, M.I., Rihs, T.A., Rochas, V., et al., 2018. From swing to cane: sex differences of EEG resting-state temporal patterns during maturation and aging. Dev. Cogn. Neurosci. 31, 58–66. https://doi.org/10.1016/j.dcn.2018.04.011.

van den Broek, S.P., Reinders, F., Donderwinkel, M., Peters, M.J., 1998. Volume conduction effects in EEG and MEG. Electroencephalogr. Clin. Neurophysiol. 106 (6), 522–534. https://doi.org/10.1016/S0013-4694(97)00147-8.

Varley, T., Craig, M., Adapa, R., et al., 2020. Fractal dimension of cortical functional connectivity networks & severity of disorders of consciousness. PLoS One 15, e0223812.

von Wegner F, Knaut P, Laufs H. EEG Microstate sequences from different clustering algorithms are information-theoretically invariant. Front Comput Neurosci. 2018;12. Accessed December 20, 2022. https://www.frontiersin.org/articles/10.3389/fncom.2018.00070.

von Wegner, F., Tagliazucchi, E., Laufs, H., 2017. Information-theoretical analysis of resting state EEG microstate sequences - non-Markovianity, non-stationarity and periodicities. Neuroimage 158, 99–111. https://doi.org/10.1016/j.neuroimage.2017.06.062.

Wang, J., Hu, X., Hu, Z., Sun, Z., Laureys, S., Di, H., 2020. The misdiagnosis of prolonged disorders of consciousness by a clinical consensus compared with repeated coma-recovery scale-revised assessment. BMC Neurol. 20, 343. https://doi.org/10.1186/s12883-020-01924-9.

Wannez, S., Heine, L., Thonnard, M., Gosseries, O., Laureys, S., 2017. The repetition of behavioral assessments in diagnosis of disorders of consciousness. Ann. Neurol. 81 https://doi.org/10.1002/ana.24962.

Whyte, J., Gosseries, O., Chervoneva, I., et al., 2009. Predictors of short-term outcome in brain-injured patients with disorders of consciousness. Prog. Brain Res. 177, 63–72. https://doi.org/10.1016/S0079-6123(09)17706-3.

Wijnen, V.J.M., van Boxtel, G.J.M., Eilander, H.J., de Gelder, B., 2007. Mismatch negativity predicts recovery from the vegetative state. Clin. Neurophysiol. 118 (3), 597–605. https://doi.org/10.1016/j.clinph.2006.11.020.

Zanesco, A.P., Denkova, E., Jha, A.P., 2021. Associations between self-reported spontaneous thought and temporal sequences of EEG microstates. Brain Cogn. 150, 105696 https://doi.org/10.1016/j.bandc.2021.105696.

Zhang, C., Yang, Y., Han, S., et al., 2023. The temporal dynamics of large-scale brain network changes in disorders of consciousness: a microstate-based study. CNS Neurosci. Ther. 29 (1), 296–305. https://doi.org/10.1111/cns.14003.